IEEE Access
Multidisciplinary | Rapid Review | Open Access Journal

Received January 9, 2019, accepted January 22, 2019, date of publication January 29, 2019, date of current version February 14, 2019.

Digital Object Identifier 10.1109/ACCESS.2019.2895626

Joint Access Mode Selection and Spectrum Allocation for Fog Computing Based Vehicular Networks

SHI YAN, XINRAN ZHANG, HONGYU XIANG, AND WENBIN WU
State Key Laboratory of Networking and Switching Technology, Beijing University of Posts and Telecommunications, Beijing 100876, China

Corresponding author: Shi Yan (yanshi01@bupt.edu.cn)

This work was supported in part by the National Science Foundation for Postdoctoral Scientists of China under Grant 2018M641279, in part by the State Major Science and Technology Special Projects under Grant 2017ZX03001014 and Grant 2018ZX03001025, and in part by the Open Research Fund of National Mobile Communications Research Laboratory, Southeast University, under Grant 2019D01.

ABSTRACT The explosive growth of data with the requirements of high reliability and low latency has posed huge challenges to the vehicular networks. One potential solution is to deploy the fog computing servers geographically closer to the vehicles to serve the vehicle-based applications in real time. However, due to the constraint of caching storage space as well as lack of tractable access mode selection and spectrum allocation algorithm, it is very challenging to balance the network transmission performance and fronthaul savings. In this paper, we investigate the joint optimization problem of access mode selection and spectrum allocation in fog computing-based vehicular networks. To solve the problem in an efficient way, the original high complexity optimization problem is divided into two subproblems. Wherein, the vehicle access mode selection problem is solved by Q-learning-based algorithm by considering spectrum allocation profiles and the fronthaul link cost. The randomly vehicular network topologies are modeled as CoX processes and the closed-form payoff expressions are derived by the stochastic geometry tools. On the other hand, the optimal spectrum allocation indicator value can be finally obtained via convex optimization. The analytical results for the proposed algorithm as well as the traditional baseline approaches are evaluated with different weight factors, which verify our theoretical analysis and confirm the proposed approach can achieve significant performance gains.

INDEX TERMS Fog computing, access mode selection, performance analysis, spectrum allocation, machine learning.

I. INTRODUCTION

To improve the road safety, traffic efficiency and entertainment experience on the wheels, the vehicular network (VNET) has been regarded as one of the key technologies in intelligent transportation system by providing the wireless connections among vehicles and remote servers [1], [2]. Compared with other various potential solutions, the cellular-based VNETs can provide ubiquitous coverage and cut down the investment by leveraging existing cellular infrastructures, decrease the end-to-end latency by introducing the direct link among vehicles, as well as provide better quality of service due to the centralized coordination of resource allocation [3], [4]. Therefore, the cellular-based VNETs have drawn much attention from both industry and academia in recent years.

Previous literatures have been done to research the performance analysis, resource allocation and mode selection in cellular-based VNETs. In [5], the handoff rate and the vehicular overhead ratio are derived to evaluate the performance of small cell based VNETs, where the distribution of small cells follows independent Poisson point processes (PPP) and the stochastic geometry tools are used to analyze the performance. Different from traditional PPP in cellular networks, Choi and Baccelli [6] modeled the locations of vehicular network nodes as a Cox point process (CPP), which can efficiently and accurately represent the coupled structure of vehicles and roads. Then, Choi and Baccelli [7] further gave a comprehensive coverage analysis of the heterogenous cellular-based VNETs. On the resource allocation and

The associate editor coordinating the review of this manuscript and approving it for publication was Guoqiang Mao.

mode selection sides, the paper [8] investigated the spectrum sharing and power allocation strategy with the latency and reliability requirements for vehicle-to-vehicle (V2V) communications with slowly varying channel information. And in [9], the outage probability and throughput are theoretically analyzed for V2V underlaid cellular networks, the impact of proposed inversion power control mechanism as well as the biased mode selection strategy on the performance is also characterized.

However, the growing demand of highly-reliable and low latency communications has became one of the huge challenges for the traditional cellular based VNETs since the limitation of the fronthaul in hotspot areas [10]. In this case, an essential question is how to find the tradeoff between the available communication resources and fronthaul cost while maintaining the profits of VNETs without compromising the network performance. Fortunately, the development of fog computing may play such kind of role. Fog computing extends computing resources and storage resources to the edge of the network [11]. It has been recognized as an indispensable part to realize the vision of future VNET applications, such as automated driving [12], [13]. In order to implement fog computing in the VNETs, the traditional base stations need to be upgraded to the fog access points (F-AP) with a edge cache storage and fog computing modules to implement the local signal processing and execute the local machine learning algorithm.

As shown in the recent studies, it has been found that integrating fog computing into cellular-based VNETs can greatly enhance the performance as well as improve the stability. In [14], multi-access edge computing (MEC) is introduced to the V2X scenario to address the automated driving use cases, the issues about MEC application programming interfaces, smart orchestration of MEC resources and the relationship with network slicing are described in detail. Huang *et al.* [15] extend the fog computing paradigm to conventional VNETs and present a high-level overview of vehicular fog computing architecture. In [16], a task-file transmission strategy with predictive V2V relay is designed, the impact of the time consumption and the offloading cost of various transmission modes on the performance is characterized. To further exploit the unoccupied resources of nearby vehicles, the paper [17] proposes a bus-based cloudlet cooperation strategy for VNETs to minimize the energy consumed by vehicles, while satisfying the completion time requirements of the applications. Hu *et al.* [18] focus on the scenario of edge caching with multiple content providers, and propose a multi-object auction-based caching strategy to improve the data dissemination for every content providers.

Despite the many promising benefits, fog computing based VNETs (FVNET) are also faced with several challenges. First, the flexibility of vehicles generally results in random network topologies which will greatly increases the difficulty of performance analysis [19]. Besides, the light-of-sight (LOS) channel and the severe interferences between other vehicles and other F-APs may drastically deteriorate the performance [20]. Finally, most of literatures only focused on the received signal to interference ratio (SIR) and distance based mode selection schemes. However, the impact of fronthaul delay and edge cache were largely ignored. In order to break through these remarkable bottlenecks for the FVNET commercial practices, a reliable access mode selection and spectrum allocation algorithm is required.

In this paper, a joint optimization problem of access mode selection and spectrum allocation algorithm is proposed for the downlink FVNETs by taking into account the random vehicular network topology, edge cache and the content download delay. Our main contributions can be summarized in three-folds.

- The coverage probability and the expected data rate of both V2V and F-AP modes are characterized, where Poisson point process and Cox point process are used to model the distribution of F-APs and vehicles, respectively. The impact of Rician channel propagations, nodes density and the cache storage size constrain are considered in the analytical results. The closed-form expressions are presented, which make the results much more tractable and flexible.
- Based on the derived analysis results, the joint optimization problem of access mode selection and spectrum allocation problem in downlink fog computing based vehicular networks is formulated, which composes two subproblems. For the formulated access mode selection subproblem, a Q-learning based algorithm is proposed to find the solution without the global information, which can reduce complexity efficiently. For the spectrum allocation subproblem, the optimal spectrum allocation indicator value can be finally obtained via convex optimization.
- The performance of the expected data rate, sum payoff, as well as the traditional baseline approaches are evaluated with different network parameters and fronthaul cost. The simulation results show that the proposed algorithms can reach the stable states very fast with a higher reward than the traditional baseline approaches.

The rest of this paper is organized as follows. Section II introduces the downlink FVNET network model, cache model, the access modes and the formulation of the optimization problem. While in Section III, the expected data rate and coverage probability for both the F-AP mode and V2V mode are derived, and a Q-learning based algorithm is proposed to solve the content require vehicles access mode selection subproblem efficiently. In Section IV, the convex optimization tools are used to obtain the optimal spectrum allocation indicator value. Simulation results have been provided in Section V, and conclusions are drawn in Section IV.

II. SYSTEM MODEL

A. VEHICLUAR NETWORK TOPOLOGY

In this paper, a downlink FVNET is considered, as illustrated in Fig. 1, the spatial distribution of vehicles are modeled by specific Cox point processes [7]. More specifically, we first

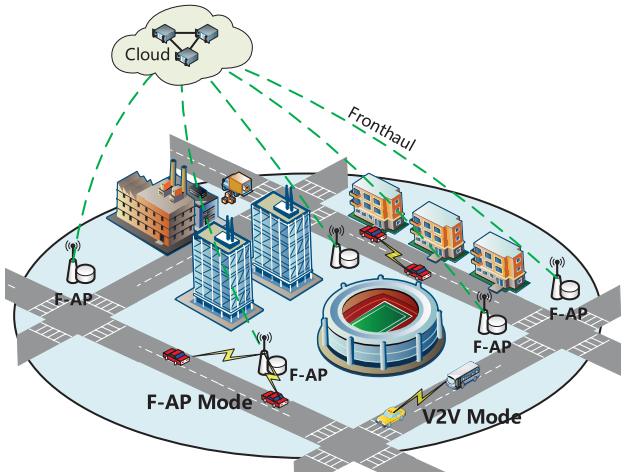

FIGURE 1. The simplified architecture of a two-tier downlink FVNET.

model the road system as a Poisson line process Φ_l with line density μ_l, which can be produced by a homogeneous PPP Ψ in the representation space $\mathcal{C} \equiv \mathbb{R} \times [0, \pi)$. The density of the equivalent point process of Ψ can be denoted as $\lambda_l \equiv \mu_l/2\pi$, and each point (r_i, θ_i) of Ψ corresponds to a line l_i with equation

$$l(r_i, \theta_i) = \{(x, y) \in \mathbb{R}^2 | x\cos(\theta_i) + y\sin(\theta_i) = r_i\}, \quad (1)$$

where θ denotes the angle from the positive x-axis to the line l, and r denotes the shortest distance between the origin and the line [7].

Then, the locations of vehicles on each line are modeled as independent one dimensional (1D) PPPs Φ_v distribution with density of λ_v. By setting the probability of a vehicle is a V2V transmit vehicle as $p \sim (0, 1]$, which means it can transmit its caching content to its nearby content require vehicle (CRV). Therefore, the V2V transmit vehicles locations can be modeled as a thinning homogeneous Φ_{tv} with the intensity $\lambda_{tv} = p\lambda_v$. Meanwhile according to Marking Theorem, the distribution of content require vehicles follows a stationary 1D PPP Φ_{rv} with the density of $\lambda_{rv} = (1 - p)\lambda_v$. Without any loss of generality, we assume the transmit vehicles are working on the same frequency band with the F-APs and the tagged content require vehicle is located at the origin. By applying Slivnyaks theorem [21], the translation of the origin can be interpreted as addition of a point at the origin to the PPP in the representation space $\mathcal{C}$. Let us denote the line containing the origin and the 1D PPP on the line by l_0 and ϕ_{l_0}, respectively, and the l_0 can be referred to as the tagged line.

On the other hand, several cache enabled F-APs are located in the area $\mathcal{D}^2$ according to a 2D PPP Φ_f with constant intensity λ_f, and connect to the cloud servers via wired fronthauls. The transmit power of each F-AP is fixed as P_f, and we assumed the F-APs are single antenna configuration. In this paper, we consider the F-APs need to share portion of their spectrum bandwidth to the transmit vehicles for V2V mode communication. Let B denote the total bandwidth size of all F-APs, and the spectrum allocation indicator β denote the portion of bandwidth size that F-APs are willing to share. We assume the content require vehicles who selected to the same access mode are shared the bandwidth, in other words, the V2V mode and F-AP mode vehicles share βB and $(1-\beta)B$ bandwidth, respectively.

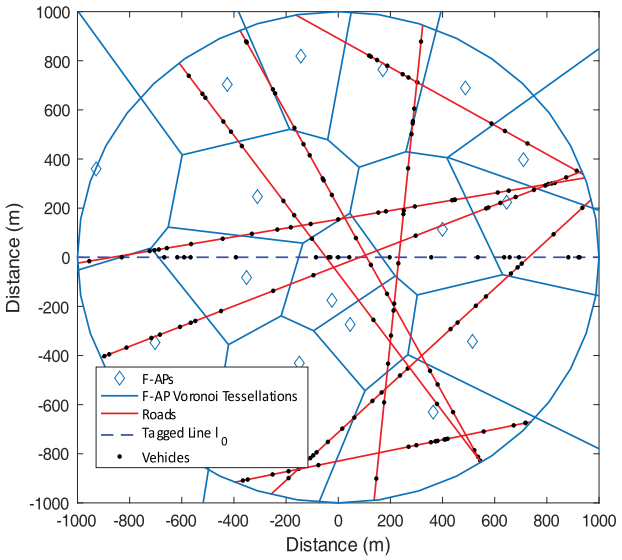

FIGURE 2. An illustration of Cox point processes, roads (line), F-APs (diamonds), and vehicles (circles).

Therefore, the collection of points is referred to as a Cox bipolar network. Fig. 2 illustrates a realization of the roads, vehicles and the Voronoi tessellation of F-APs, where the radius of the disc plane is $1km$, the density of F-APs is $\lambda_f = 5/km^2$ and the density of roads and vehicles is $\lambda_l = 10/2\pi/km$ and $\lambda_v = 10/km$, respectively.

B. CACHE MODEL

In this FVNET, the F-APs can cache multiple content files from the centralized cache library in the cloud sever, which stores N contents $\mathcal{N} \equiv \{1, 2, ..., N\}$ that may be requested by users [22]. Without loss of generality, each content v has a fixed size C_f. Then, the transmit vehicles will storage a portion of the content from F-APs through wireless communication. We set C_f and C_v ($C_v < C_f < N$) denote the limited local cache size of the F-APs and V2V transmit vehicles, respectively, and assume the contents in C_f and C_v are fixed for a long time interval.

In the previous literatures, it has been researched that the users are mostly interested in downloading the most popular contents [23]. In other words, the majority of users only frequently requested a small part of the contents. Therefore, the F-APs and V2V transmit vehicles are assumed only store the contents with the most popularity in this paper, and the Zipf distribution can be used to model the demand probability

$$f_j(N, \sigma) = \frac{1/j^\sigma}{\sum_{i=1}^{N} 1/i^\sigma}, \quad (2)$$

where $\sigma > 0$ is the Zipf exponent, it controls the relative popularity of files, and $\sum_{i=1}^{N} f_i(N,\sigma) = 1$, $f_a(N,\sigma) > f_b(N,\sigma)$, if $a < b$.

Therefore, the caching probability can be defined as the probability that a content require vehicle V can download its requested content n from the associated node, i.e., $p_c^x = \Pr(n \in C_x)$. Let F-APs and V2V transmit vehicles only store the most popularly requested contents in their local caching, then the caching probabilities of V2V transmit vehicles and F-APs can be denoted as

$$p_c^f = \Pr(n \in C_f) = \sum_{i=1}^{C_f} f_i(\sigma, N), \tag{3}$$

$$p_c^v = \Pr(n \in C_v) = \sum_{i=1}^{C_v} f_i(\sigma, N). \tag{4}$$

C. ACCESS MODES

In this paper, we consider two mode selection for content require vehicles, named: V2V mode and F-AP mode. A CRV can select an access mode independently by take into account both of the network performance payoff and its delay cost. Let $V \to X$ denotes that a tagged CRV V selects to access a node located on X, and the distance from V to X can be expressed as $\|X\|$. By using the property of Cox process, the number of CRVs can be estimated as $N_{rv} = \mathcal{P}(\mathcal{D}^2)(1-p)\lambda_v\lambda_l\mathbb{E}[l]$, where $\mathcal{P}(\mathcal{D}^2)$ is the perimeter of the disc plane $\mathcal{D}^2$ and $\mathbb{E}[l]$ denotes the mean line length. The definitions of two access modes are given as follows:

- **V2V mode:** A CRV selects V2V mode if it can direct download the requested content from a V2V transmit vehicle, where the transmit vehicle is located in a distance constraint L_v.
- **F-AP mode:** A CRV selects F-AP mode if the vehicle cannot find a V2V transmit vehicle in the distance constraint L_v, or the V2V transmit vehicle do not has the requested content V. Therefore, V need to select to its nearest F-AP.

Similar to other literatures, if a CRV selects V2V mode, a wireless link will be established between the CRV and its service transmit vehicle. Then, the CRV will receive the content without utilization of fronthaul. However, if the CRV cannot find its content in the transmit vehicle, it needs to switch to the F-AP mode. On the other hand, if a CRV associated with a F-AP that the F-AP stores the desired content in its cache, the F-AP will send the content file to the CRV directly. Otherwise, the CRV needs to download the file from the cloud server with an additional fronthaul load.

Let p_v signify the probability of at least one V2V transmit vehicle can be found within the constraint L_v meanwhile cached the content V that the CRV requested. By using some properties of 1-D PPP, we can easily obtain the distribution of the nodes number in a line with length limit 2 L_v, which are given as follows

$$p_v = 1 - \exp(-2\lambda_{tv} p_c^v L_v). \tag{5}$$

Then, the number of potential F-AP and V2V mode vehicles can be obtain as $N^{(F)} = N_{rv}(1-p_v)$ and $N^{(V)} = N_{rv}p_v$, respectively.

D. PROBLEM FORMULATION

The global objective is to find the optimal joint access mode selection and spectrum allocation profile that maximize the expected payoff of the network. The logarithmic function is used to model the payoff function, and it has proven the logarithmic objective function is maximized if the resource is equally shared among the users [24] [25]. Therefore, the considered problem can be formulated as

$$\mathcal{P}_1 : \max_{x,\beta} \sum_{s\in\mathcal{S}} \sum_{k=1}^{N_{rv}} x_{sk} \log\left(\frac{p_s B_s(\beta) R_s}{\sum_{k=1}^{N_{rv}} x_{sk} C_s}\right), \tag{6}$$

$$\text{s.t.} \sum_{s\in\mathcal{S}} x_{sk} = 1, \forall k, \mathcal{S} \equiv \{v, f\} \tag{7}$$

$$\sum_{k=1}^{N_{rv}} x_{sk} = N_s, s \in \mathcal{S}, \tag{8}$$

$$N_v \le N^{(V)}, \tag{9}$$

$$x_{sk} \in \{0,1\}, 0 \le \beta \le 1, \tag{10}$$

where x_{sk} denotes the access mode selection indicator, which is a binary variable. R_s represents the expected data rate of a CRV choosing to associate with access mode s, which will be further discussed in Section III. p_s is a linear price function charged by the vehicles in access mode s. $B_v(\beta) = \beta B$ and $B_f(\beta) = (1-\beta)B$ are the allocated bandwidth of V2V mode and F-AP mode, respectively. Constraint (7) implies that each CRV only can select one access mode. Constraint eqrefp13 indicates the number of the CRVs served by the V2V and F-AP mode. Constraint (9) represents the number limit of potential V2V mode vehicles. C_s is the cost function that is related to whether the content v is cached in mode s, which can be further represented as

$$C_s = \begin{cases} D_v, & V2V\ mode, \\ D_f + (1-p_c^f)D_{\mathcal{F}}, & FAP\ mode. \end{cases} \tag{11}$$

where constants D_v and D_f denote the cache processing cost price of V2V and F-AP, respectively, which mainly come from the cache data processing. $(1-p_c^f)D_{\mathcal{F}}$ is the F-AP fronthaul cost price.

The above optimization problem is a mixed-integer nonlinear programming (MINLP) problem since the access mode selection indicator x_{sk} is a binary variable and standard optimization techniques cannot be applied directly. Meanwhile, the payoff function will be affected by both the number of CRVs choosing the same access modes and the spectrum allocation profile, which can in turn affects the F-APs bandwidth partition decision. To solve the optimization problem in an efficient way, the primary problem $\mathcal{P}_1$ can be divided into two subproblems: access mode selection subproblem with given spectrum allocation profile, and a spectrum allocation subproblem for fixed CRV association states. Wherein, each CRV needs to select an access mode (i.e. V2V mode or F-AP mode) for payoff maximization which depends on both of the expected data rate and the fronthaul cost. While F-APs need to decide how much bandwidth allocation to the V2V

communications by considering the status of access mode selection. Then, an iterative algorithm is proposed to solve the original problem. In the following, by using stochastic geometry and machine learning tools, the access mode selection subproblem is investigated in Section III. Soon afterwards the spectrum allocation subproblem is studied in Section IV.

III. ACCESS MODE SELECTION SUBPROBLEM

The network payoff expressions for both V2V and F-AP mode are derived in this section through the stochastic geometry tool. Then, a Q-learning algorithm based solution for the access mode selection subproblem is given with fixed spectrum allocation profiles.

A. FORMULATION OF THE ACCESS MODE SELECTION SUBPROBLEM

We first fixed the spectrum allocation indicator β, then the access mode selection optimization subproblem can be rewritten as follows

$$\mathcal{P}_2: \max_{x} \sum_{s\in\mathcal{S}}\sum_{k=1}^{N_{rv}} x_{sk}\log\left(\eta_s R_s\right) - \sum_{s\in\mathcal{S}} N_s \log\left(N_s\right), \tag{12}$$

$$\text{s.t.} \sum_{s\in\mathcal{S}} x_{sk} = 1, x_{sk}\in\{0,1\}, \forall s,k, \tag{13}$$

$$\sum_{k=1}^{N_{rs}} x_{sk} = N_s, s\in\mathcal{S}, \tag{14}$$

$$N_v \le N^{(V)}, \tag{15}$$

where (12) is rewritten from (6), and $\eta_s = p_s B_s(\beta)/C_s$.

Next, we will derive the expected data rate performance R_s expressions presented in the above subproblem for both F-AP and V2V modes by considering the different network parameters.

B. PERFORMANCE ANALYSIS

In this subsection, the stochastic geometry tool is used to derive the expected data rate performance with two different access modes. Since the interference is much stronger than the noise, the interference-limited scenario is considered in this paper. The radio channel is assumed to be a combination of standard pathloss propagation and small-scale fast fading. The standard pathloss propagation can be denoted as $\|X\|^{-\alpha}$, where $\|X\|$ is the distance between the typical CRV and its associated node, and $\alpha > 2$ is the pathloss exponent. By considering the LOS component is much more prominent for the V2V communications, the small-scale fast fading is assumed as the Rician fading [26]. According to prior studies, the probability density function (PDF) of the Rician fading can be molded as a scaled non-central chi-squared distribution with two degrees of freedom

$$f_x(x) = (1+K)\, e^{-K-(1+K)x} I_0\left(2\sqrt{K(1+K)x}\right), \tag{16}$$

where $I_0(\cdot)$ denoted the modified Bessel function of the first kind and zero order. K is the Rician factor, denoting the ratio of the power of the LOS component over that of the scattered components.

We focus on the V2V mode first. Let set the tagged CRV is accessed to a V2V transmit vehicle with a distance $\|X_v\|$ between them. Then, the CRV received SIR can be given as

$$SIR(V\to X_v) = \gamma_v = \frac{P_v h_v \|X_v\|^{-\alpha}}{I_{l_0,rv} + I_{v,rv} + I_{f,rv}}, \tag{17}$$

where h_v characterizes the Rician channel from the tagged CRV and the transmit vehicle, and $\|X_v\|^{-\alpha}$ denotes the path loss. $I_{v,rv} = \sum_{X_i\in\Phi_{tv}} P_v g_i \|X_i\|^{-\alpha}$ is the inter-road interference from the transmit vehicles in the other roads. $\|X_i\|^{-\alpha}$ and $g_i \sim \exp(1)$ denote the path loss and the exponentially distributed Rayleigh channel fading from other V2V transmit vehicles to V, respectively. $I_{l_0,rv} = \sum_{X_i'\in\phi_{l_0}} P_v g_i' \|X_i'\|^{-\alpha}$ denotes the interference from other V2V transmit vehicles in the same road (i.e. the tagged line l_0). $I_{f,rv} = \sum_{X_j\in\Phi_f} P_f g_j \|X_j\|^{-\alpha}$ denotes inter-tier interference from F-APs. The definition of g_j and $\|X_j\|^{-\alpha}$ are similar to that in $I_{v,rv}$.

Next, if the tagged CRV selects F-AP mode and access to its nearest F-AP, the SIR of V can be given as

$$SIR(V\to X_f) = \gamma_f = \frac{P_f h_f \|X_f\|^{-\alpha}}{I_{l_0,fv} + I_{v,fv} + I_{f,fv}}, \tag{18}$$

where $I_{f,fv} = \sum_{X_j'\in\Phi_f/f} P_f g_j' \|X_j'\|^{-\alpha}$ denotes the interference from other F-APs in this network, $I_{v,fv} = \sum_{X_k\in\Phi_{tv}} P_v g_k \|X_k\|^{-\alpha}$ and $I_{l_0,fv} = \sum_{X_k'\in\phi_{l_0}} P_v g_{k'} \|X_k'\|^{-\alpha}$ represent the inter-road interference from V2V vehicles in other roads, and the inter-road interference from V2V vehicles in the same road, respectively. The definitions of channel fading h and g, as well as the distance $\|X\|$ are similar to that in (17).

1. V2V mode performance

In V2V mode, the closed-form coverage probability of the tagged CRV can be obtained as

$$\begin{aligned} P_v(T_v,\alpha,K,\|X_v\|) &= \Pr\left(\gamma_v > T_v\right) \\ &\approx \sum_{i=1}^{N_K} w_i^K \exp\left(-2\lambda_{tv}\|X_v\|\left(u_i^K T_v\right)^{\frac{1}{\alpha}}\Delta'(\alpha)\right) \\ &\cdot \exp\left(-\lambda_{tv}\lambda_l\pi^2\|X_v\|^2\left(u_i^K T_v\right)^{\frac{2}{\alpha}}\Delta(\alpha)\right) \\ &\cdot \exp\left(-\lambda_f\pi\|X_v\|^2\left(P_f u_i^K T_v/P_v\right)^{\frac{2}{\alpha}}\Delta(\alpha)\right), \end{aligned} \tag{19}$$

where, $\Delta'(\alpha) = \pi\csc(\pi/\alpha)/\alpha$ and $\Delta(\alpha) = 2\pi\csc(2\pi/\alpha)/\alpha$.

Proof: See Appendix A. ■

Then, according to the definition [27] [28], the expected data rate performance of V2V mode can be obtained as

$$R_v(T_v,\alpha,K,\|X_v\|) = P_v(T_v,\alpha,K,\|X_v\|)\log(1+T_v). \tag{20}$$

2. F-AP mode performance

If the tagged CRV select to F-AP mode,it will access to the near by F-AP X_j to obtain its requested content. The PDF of the distance between X_j and the tagged vehicle V can be given as $f_{\|X_f\|}(r_f) = 2\pi\lambda_f r_f \exp\left(-\pi\lambda_f r_f^2\right)$ [22]. Thus, the closed-form coverage probability of F-AP mode can be calculated as

$$P_f\left(T_f,\alpha\right) = \Pr\left(\gamma_v > T_v\right) = c\left\{\frac{1}{2b} + \frac{a\sqrt{\pi}e^{-a^2/4b}}{4b^{3/2}}\left[erf\left(\frac{a}{2\sqrt{b}}\right) - 1\right]\right\}, \tag{21}$$

where the terms in (21) are $a = 2\lambda_{tv}\Delta'(\alpha)\left(T_f P_v/P_f\right)^{1/\alpha}$, $b = \pi\lambda_f\left(1+\rho\left(T_f,\alpha\right)\right) + \pi^2\lambda_{tv}\lambda_l\left(T_f P_v/P_f\right)^{2/\alpha}\Delta(\alpha)$, $c = 2\pi\lambda_f$, and $\rho\left(T_f,\alpha\right) = \int_{T_f^{-2/\alpha}}^{\infty}\frac{T_f^{2/\alpha}}{1+v^{\alpha/2}}dv$.

Proof: See Appendix B. ∎

And the the expected data rate performance of F-AP mode can be given as

$$R_f(T_f,\alpha) = P_f(T_f,\alpha)\log(1+T_f). \tag{22}$$

C. Q-LEARNING ALGORITHM BASED SOLUTION

In this subsection, we present a Q-learning algorithm to find the solution of the access mode selection subproblem. In this algorithm, Q-value is used to maintain the knowledge about each access node, and the decision can be made based on this knowledge.

First, we define the related space and reward of the Q-learning algorithm as follows

- **State Space $\mathcal{X}$:** we redefine x_{sk} denotes the access mode selection state of the CRV k. Therefore, the mode selection state of all N_{rv} vehicles can be represented as a vector $x = \left[x_1, x_2, ..., x_{N_{rv}}\right]$. Considering the vehicle may change its decision and switch to another mode many times at each decision point, we finally list the state space as $\mathcal{X} = \{x_0, x_1, ..., x_i, ...\}$.
- **Action Space $\mathcal{A}$:** In order to reduce the complexity, the action space for a vehicle is defined as $\mathcal{A} = \{a_1, a_2, ..., a_i, ...\}$. At a epoch i in a decision point, each vehicle determines to select the action $a_i \in \{-1, 0, 1\}$ according to its current state x_i. More specifically, If $a_i = -1$, the next state would be x_{i-1}. If $a_i = 0$, the next state will remain in the same state x_i. If $a_i = 1$, then, the state will jump to x_{i+1}.
- **Reward π_i:** The reward quantifies the performance satisfaction level which depends on the expected data rate as well as the cost. In this paper, the immediate reward in internal i is defined as follows:

$$\pi_i = \sum_{s\in\mathcal{S}}\sum_{k=1}^{N_{rv}} x_{sk}\log\left(\eta_s R_s\right) - \sum_{s\in\mathcal{S}} N_s\log\left(N_s\right). \tag{23}$$

In each epoch i of the mode select decision point, each CRV chooses the action with the highest estimated Q value with probability $1-\varepsilon$, or a random action from the action set with probability ε. After selecting and executing action a_i^*, the immediate reward π_i and next state $\boldsymbol{s}_{i+1}$ from the FVNET are observed. Then, the association state transition $(\mathbf{s}_i; a_i; \pi_i; \mathbf{s}_{i+1})$ will send to the F-APs, and the Q value is updated. The speed of adjustment of the Q-value is controlled by a parameter $\zeta > 0$ and η denotes the future discount factor. Hence, we could derive the user association algorithm as described in Algorithm 1.

Algorithm 1 Q-learning Algorithm

1: **Initialize** Initialize action-value function $Q(\mathbf{s}, a)$.
2: **Loop**
3: **if** $rand() \le \varepsilon$
4: Content require vehicle selects an random action from the action set.
5: **else**
6: Content require vehicle chooses the action with the highest estimated Q value, $a_i^* = \arg\max Q\left(\mathbf{s}_i, a_i\right)$.
7: **end if**
8: Content require vehicle computes the reward π_i.
9: Update the new Q value with $Q(\mathbf{s}_{i+1}, a') = (1-\zeta)Q(\mathbf{s}_i, a) + \zeta\left(\pi_i + \eta\arg\max Q\left(\mathbf{s}_i, a_i\right)\right)$.
10: **end loop** until convergence.

IV. SPECTRUM ALLOCATION SUBPROBLEM

In Section III, a Q-learning based algorithm for access mode selection is proposed and the algorithm details are described. After all of the CRVs adjust their strategies, the behavior of the access mode selection reaches the fixed status. Based on the status, the solution of the spectrum allocation subproblem is given in this section.

A. FORMULATION OF SPECTRUM ALLOCATION SUBPROBLEM

When the access mode selection indicator x_{sk} is fixed, the spectrum allocation subproblem can be formulated as

$$\mathcal{P}_3: \max_{\beta}\sum_{k=1}^{N_{rv}} x_{vk}\log\left(\beta\varepsilon_v\right) + \sum_{k=1}^{N_{rv}} x_{fk}\log\left((1-\beta)\varepsilon_f\right), \tag{24}$$

$$\text{s.t.} \quad 0 \le \beta \le 1, \tag{25}$$

where $\varepsilon_v = p_v B_v R_v/(C_v N_v)$, and $\varepsilon_f = p_f B_f R_f/(C_f N_f)$.

Firstly, We denote the right side of (24) as F. Therefore, the second order derivative of F with respect to β can be derived as

$$\frac{\partial^2 F}{\partial\beta^2} = -\frac{\sum_{k=1}^{N_{rv}} x_{vk}}{(1-\beta)^2} - \frac{\sum_{k=1}^{N_{rv}} x_{fk}}{\beta^2}. \tag{26}$$

It is obvious that for any $x > 0$ and $0 \le \beta \le 1$, we have $\frac{\partial^2 f}{\partial\beta^2} < 0$. Then, the spectrum allocation can be proofed as convex, since the original subproblem has a linear constraint (25). Therefore, we can obtain the optimal value

of β by letting the first order derivative of f equals to zero. Then, the optimal β can be expressed as

$$\beta^* = \frac{\sum_{k=1}^{N_{rv}} x_{fk}}{\sum_{k=1}^{N_{rv}} x_{fk} + \sum_{k=1}^{N_{rv}} x_{vk}}. \quad (27)$$

Then, the formulated joint access mode selection and spectrum allocation problem in Section II can be solved with the iterative algorithm, which can be summarized as Algorithm 2.

Algorithm 2 Joint Access Mode Selection and Spectrum Allocation Algorithm

1: **Initialize** Initialize spectrum allocation indicator $\beta = 0.5$, and solve the initial mode selection problem according to Algorithm 1.
2: **Loop**
3: For fixed access mode selection indicator x_{sk}, calculate the optimal spectrum allocation indicator β^* by using (27).
4: Update the new optimal access mode selection indicator with fixed β^*
5: **end loop** until convergence.

V. NUMERICAL RESULTS

In this section, the analytical results for the proposed algorithm as well as the traditional baseline approaches are evaluated with different network parameters. The key simulation parameters are listed as follows in Table 1.

TABLE 1. Simulation parameters.

Parameters	Value
The radius of the area	1km
Intensity of F-APs λ_f	5×10^{-6}
Intensity of roads λ_l	$5 \times 10^{-3}/\pi$
Intensity of transmit vehicles λ_{tv}	1×10^{-2}
The distance between the typical V2V pair $\|X_v\|$	50m
Path loss exponent α	4
Transmit power of transmit vehicles P_v	23dBm
Transmit power of F-AP P_f	33dBm
Number of video content N	50000
Total bandwidth of F-APs	100MHz

A. PERFORMANCE OF ACCESS MODE SELECTION

Monte Carlo simulation method is used in this subsection to evaluate the accuracy of the performance expressions for both V2V and F-AP modes in Section III. Then, we illustrate the performance improvement of the proposed Q-learning based access mode selection algorithm. The values of the Rician fading coefficients u_i^K and w_i^K, mainly borrowed from [29], are shown in Table 2.

Fig. 3 shows the coverage probability achieved by the V2V mode with different Rician fading factors K versus the varying SIR thresholds T_v. As shown in Fig. 3, the coverage

TABLE 2. Ricain fading simulation parameters.

Term	$K=1$		$K=5$		$K=10$	
Index	w_i^K	u_i^K	w_i^K	u_i^K	w_i^K	u_i^K
$i=1$	-0.8993	1.2475	42.253	2.9576	177.75	3.8741
$i=2$	5.9324	1.4298	-189.99	3.7559	-338.04	4.3761
$i=3$	-5.4477	1.7436	192.97	4.1436	297.00	5.3985
$i=4$	1.4145	2.0326	-44.229	4.7715	-135.71	5.9937

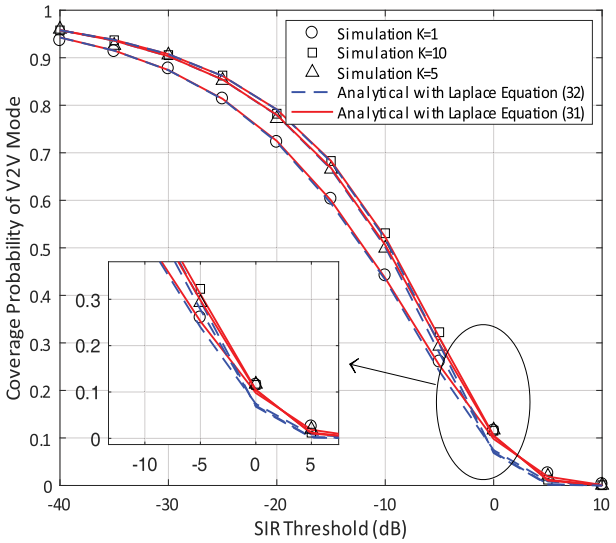

FIGURE 3. The coverage probability of V2V mode versus different SIR thresholds.

probability of V2V mode increases with an increasing Rician factor K, this is because Rician fading factors is defined as the ratio of the power in the dominant component to the average power in the diffuse components. Thus, a higher K means the CRV receives more transmission power from its nearest transmit vehicle directly. We also compare the Monte Carlo simulation results with the exact analytical result (i.e. Laplace transform according to Equation (31)) and the approximate analytical result (i.e. Laplace transform according to Equation (32)). It can be observed that in Fig. 3, both the exact and approximate analytical results are consistent with the Monte Carlo simulation results in the vast majority of the coverage probability, and the approximate analytical result exists small gap (within a few percent) when the coverage probability is lower than 0.1, which confirms our theoretical analysis.

From Fig. 4, it can be observed that the expect data rate performance in V2V mode is better than F-AP mode, since the V2V communication with a closer distance can effectively improve the system performance. In addition, the expect data rates of V2V mode decrease monotonically as the distance between the transmit and CRV $\|X_v\|$ increases. This is because that the larger $\|X_v\|$ means the pathloss become larger, which lead the performance worse. On the other hand, with the SIR threshold increases, the rate performance of both the V2V and F-AP mode increases first

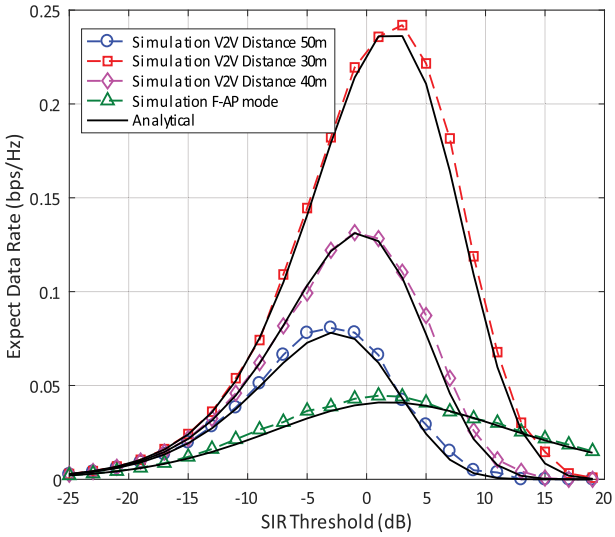

FIGURE 4. Expect data rate of V2V mode and F-AP mode versus different SIR thresholds.

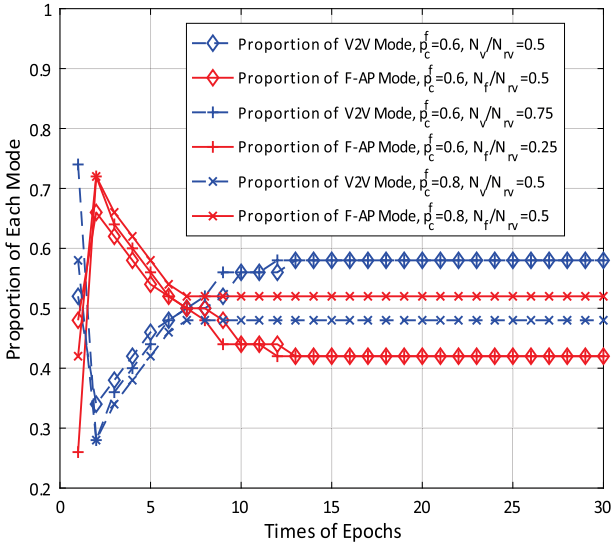

FIGURE 5. Proportion of CRV with the access mode selection algorithm (N_s/N_{rv}).

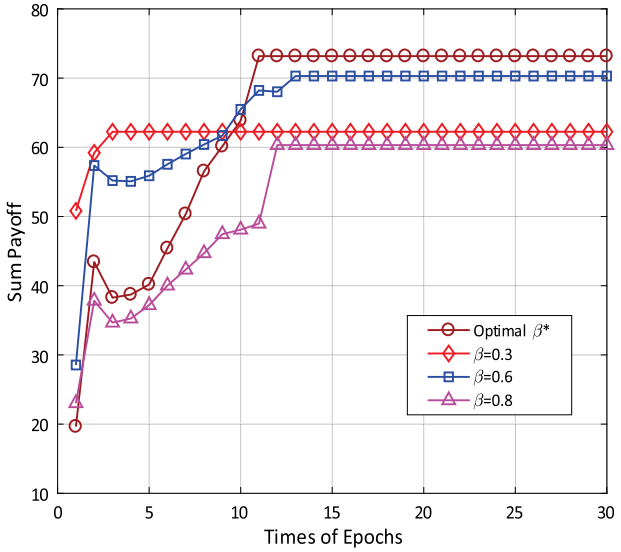

FIGURE 6. The sum payoff with different spectrum allocation indicator β.

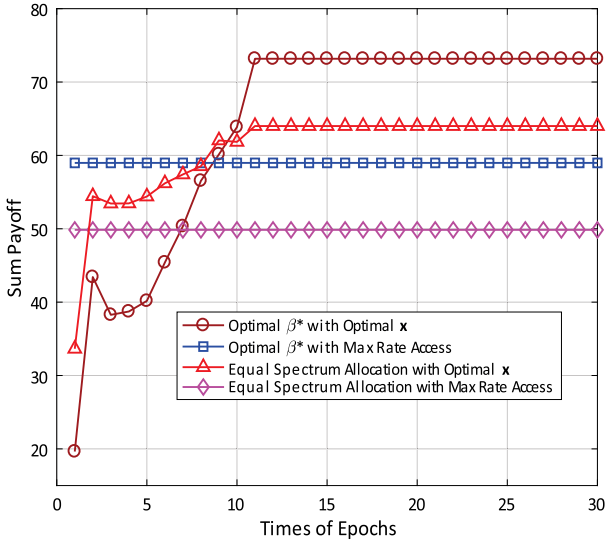

FIGURE 7. The sum payoff with different access mode selection and spectrum allocation algorithm.

and then decreases. This is because the larger SIR threshold suggests the $\log(1+T)$ increases but the coverage probability becomes smaller. The mixed influences lead to that the expect data rate is a concave function of T and there is an optimal SIR threshold making the rate performance achieve the maximized value.

The trajectories of the proportion per CRV accessing different access modes during the Q-learning algorithm are shown in Fig. 5. It can be observed in Fig. 5, our proposed algorithm can reach the stable states within around 15 times of epochs. On the other hand, it can be found that after several iterations all curves with different initial proportion (i.e. 50% and 75% CRV selecting V2V mode at the initial point) at last converge to the same stable state after changing in different directions.

On the other hand, it can be observed that the F-APs with higher F-AP content caching probability (i.e. p_c^f changes from 0.6 to 0.8) will attract more CRVs to select F-AP mode. This is because a higher content caching probability means the CRV selects to F-AP mode can reduce its download delay cost.

B. PERFORMANCE OF SPECTRUM ALLOCATION

In this subsection, the performance of spectrum allocation algorithm in Section IV is shown through the MATLAB platform simulation. Without loss of generality, the popularity of the content requested by the user follows the Zipf distribution with a parameter of 0.8. The content caching probability of

transmit vehicles and F-APs are $p_c^v = 0.4$ and $p_c^f = 0.6$, respectively.

Fig. 6 describes the relationship between the sum payoff and different spectrum allocation indicators β. It can be observed that after several iterations all curves with different spectrum allocation indicators at last achieve a much better sum payoff. Moreover, the sum payoff with the optimal spectrum allocation indicator outperforms other spectrum allocation schemes. At the same time, those curves about access mode selection finally converge to the stable states.

We compare the performance of the proposed algorithm with different access mode selection and spectrum allocation algorithms in Fig. 7. From Fig. 7, the proposed joint access mode selection and spectrum allocation algorithm achieves a much better performance than other algorithms. More specifically, the proposed algorithm can improve by as much as 15% and 25% on the equal allocation schemes and the max rate based access mode selection schemes.

VI. CONCLUSION

In this paper, we have investigated joint access mode selection and spectrum allocation problem in FVNETs. With the difference of vehicles performances and the the limitation of delay cost considered, a MINLP optimization problem is formulated. To solve this high complexity problem efficiently, we divided the original problem into two subproblems. Stochastic geometry is used to model the distribution of vehicles and network nodes, and derive the reward expressions of access mode selection by taking into account the locations of F-APs, roads and vehicles, as well as other network parameters. For the access mode selection subproblem, we have designed a machine learning based algorithms to find the stable state. For the spectrum allocation subproblem, we can finally obtain the optimal spectrum allocation indicator value. The simulation results confirm the validity of our analysis, and show the proposed algorithms can reach the stable state with a higher reward than the traditional baseline algorithms.

APPENDIX

A. PROOF OF $P_V(T_V, \alpha, K, \|X_V\|)$

The coverage probability is defined as the probability of SIR γ_v between the two V2V mode vehicles larger than a SIR threshold T_v. Therefore, according to this definition, we can drive the coverage probability of V2V mode as

$$\begin{aligned} P_v(T_v, \alpha, K, \|X_v\|) &= \Pr\left(\frac{P_v h_v \|X_v\|^{-\alpha}}{I_{l_0,rv} + I_{v,rv} + I_{f,rv}} \geq T_v\right) \\ &= \Pr\left(h_v \geq \frac{T_v \|X_v\|^{\alpha}}{P_d}\left(I_{l_0,rv} + I_{v,rv} + I_{f,rv}\right)\right) \\ &\overset{(a)}{\approx} \mathbb{E}\left[\sum_{i=1}^{N_K} w_i^K \exp\left(-\frac{u_i^K T_v \|X_v\|^{\alpha}}{P_v}\left(I_{l_0,rv} + I_{v,rv} + I_{f,rv}\right)\right)\right] \\ &\overset{(b)}{=} \sum_{i=1}^{N_K} w_i^K \mathcal{L}_{I_{l_0,rv}}(\delta)\, \mathcal{L}_{I_{v,rv}}(\delta)\, \mathcal{L}_{I_{v,rv}}(\delta), \end{aligned} \tag{28}$$

where (a) follows the PDF of Rician fading in Equation (16) can be further estimated as a weighted sum of multiple exponential functions [29]

$$f_x(x) \approx h(x) = \sum_{i=1}^{N_K} w_i^K e^{-u_i^K x}, x \in [0, W], \tag{29}$$

where N_K is the number of terms in the exponential series which is related to the Rician factor K. Both w_i^K and u_i^K are the real coefficients of the n^{th} term under the constraints $u_i^K > 0$ and $\sum_{i=1}^{N_K} w_i^K = 1, i = 1, 2, ..., N_K$, and $[0, W]$ is the range of interest for x.

The step (b) in (28) follows from letting $\delta = u_i^K T_v \|X_v\|^{\alpha}/P_v$ in the Laplace transforms of $I_{l_0,rv}$, $I_{v,rv}$, and $I_{f,rv}$. Using the definition of the Laplace transform we can get

$$\begin{aligned} \mathcal{L}_{I_{l_0,rv}}(\delta) &= \mathbb{E}\left[\prod_{X_i' \in \phi_{l_0}} \exp\left(-\delta P_v g_i' \left\|X_i'\right\|^{-\alpha}\right)\right] \\ &\overset{(a)}{=} \exp\left(-\int_0^{\infty} \mathbb{E}_{g_i'}\left[1 - e^{\delta P_v g_i' \|X_i'\|^{-\alpha}}\right] \lambda_{tv}\left(\left\|X_i'\right\|\right) d\left\|X_i'\right\|\right) \\ &\overset{(b)}{=} \exp\left(-\lambda_{tv} B(d) \mathbb{E}\left[{g_i'}^{d/\alpha}\right] \Gamma(1 - d/\alpha) (\delta P_v)^{d/\alpha}\right) \\ &\overset{(c)}{=} \exp\left(-2\lambda_{tv} (\delta P_v)^{1/\alpha} \Delta'(\alpha)\right), \end{aligned} \tag{30}$$

where (a) follows the expectation over g_i' can be moved inside the product since the fading is assumed independent of the point process, (b) follows from probability generating functional (PGFL) of PPP [30] and $\lambda_{tv}\left(\left\|X_i'\right\|\right) = d\lambda_{tv} B(d) \left\|X_i'\right\|^{d-1}$, here d is the dimensional of the point process ($d = 1$ for Φ_{l_0}), $B(d) = |B(o, 1)|$ is the volume of the d-dimensional unit ball ($B(1)$=2 for $d = 1$), (c) results from algebraic manipulation after using some properties of Gamma function and for Rayleigh fading we can get $\mathbb{E}\left[{g_i'}^{1/\alpha}\right] = \Gamma(1 + 1/\alpha)$.

Next, the Laplace transform of $I_{v,rv}$ can be derived as

$$\begin{aligned} \mathcal{L}_{I_{v,rv}}(\delta) &= \mathbb{E}\left[\prod_{X_i \in \Phi_{tv}} \exp\left(-\delta P_v g_i \|X_i\|^{-\alpha}\right)\right] \\ &\overset{(a)}{=} \prod_{r_i \in \Psi} \mathbb{E}\left[\prod_{t_j \in \Phi_{l(r_i,\theta_i)}} \exp\left(-\delta P_v g_i \left(r_i^2 + t_j^2\right)^{-\frac{\alpha}{2}}\right)\right] \\ &\overset{(b)}{=} \prod_{r_i \in \Psi} \exp\left(-2\lambda_{tv} \int_0^{\infty} \frac{\delta P_v \left(r_i^2 + v^2\right)^{-\alpha/2}}{1 + \delta P_v \left(r_i^2 + v^2\right)^{-\alpha/2}} dv\right) \\ &\overset{(c)}{=} \exp\left(2\pi\lambda_l \int_0^{\infty} 1 - e^{-2\lambda_{tv} W(u)} du\right), \end{aligned} \tag{31}$$

where (a) follows the Euclidean distance of a transmit vehicle on line l to the tagged CRV located on the origin, (b) follows from the PGFL formula for the 1D PPP on each line l (r_i, θ_i), and (c) follows from the PGFL of 2D PPP representing the line process Ψ in the representation space [31] and setting $W(u) = \int_0^{\infty} \frac{\delta P_v \left(u^2 + v^2\right)^{-\alpha/2}}{1 + \delta P_v \left(u^2 + v^2\right)^{-\alpha/2}} dv$.

Then, using the Taylor series expansion of exponential function $\exp(x) = 1 + \sum_{a=1}^{\infty} \frac{x^a}{a!}$, the (31) can be further derived as

$$\begin{aligned}\mathcal{L}_{I_{v,rv}}(\delta) &= \exp\left(2\pi\lambda_l \int_0^{\infty} \sum_{a=1}^{\infty} \frac{(2\lambda_{tv} W(u))^a}{a!} du\right) \\ &\overset{(a)}{\approx} \exp\left(2\pi\lambda_l \int_0^{\infty} 2\lambda_{tv} W(u) du\right) \\ &\overset{(b)}{=} \exp\left(2\pi\lambda_l \int_0^{\frac{\pi}{2}} 2\lambda_{tv} \int_0^{\infty} \frac{\delta P_v \|X_i\|^{-\alpha+1}}{1+\delta P_v \|X_i\|^{-\alpha}} d\|X_i\| d\theta\right) \\ &\overset{(c)}{=} \exp\left(2\pi^2\lambda_l\lambda_{tv} \frac{(\delta P_v)^{2/\alpha}}{2} \int_0^{\infty} \frac{1}{1+w^{\alpha/2}} dw\right) \\ &\overset{(d)}{=} \exp\left(-pi^2\lambda_l\lambda_{tv} (\delta P_v)^{2/\alpha} \Delta(\alpha)\right), \end{aligned} \tag{32}$$

where (a) follows from the value of $2\lambda_{tv}W(u)$ is small enough that the integrand can be evaluated to 0 for all $a > 1$, (b) results from switch Cartesian to polar coordinates, and using some algebraic simplified methods. (c) follows from setting $w = \|X_i\|^2 / (\delta P_v)^{2/\alpha}$ and (d) follows from using some properties of Gamma function.

Finally, the Laplace transform of $I_{f,rv}$ can be obtained in a similar way as $I_{l_0,rv}$

$$\begin{aligned}\mathcal{L}_{I_{f,rv}}(\delta) &= \mathbb{E}\left[\prod_{X_j\in\Phi_f} \exp\left(-\delta P_f g_j \|X_j\|^{-\alpha}\right)\right] \\ &= \exp\left(-\int_0^{\infty} \mathbb{E}_{g_j}\left[1 - e^{\delta P_f g_j' \|X_j\|^{-\alpha}}\right] \lambda_f\left(\|X_j\|\right) d\|X_j\|\right) \\ &\overset{(a)}{=} \exp\left(-\lambda_f B(2) \mathbb{E}\left[{g_j}^{2/\alpha}\right] \Gamma(1-2/\alpha) \left(\delta P_f\right)^{d/\alpha}\right) \\ &\overset{(b)}{=} \exp\left(-\pi\lambda_f \left(\delta P_f\right)^{2/\alpha} \Delta(\alpha)\right), \end{aligned} \tag{33}$$

where (a) is from the PGFL of 2D PPP Φ_f and the volume of the 2-dimensional unit ball $B(2) = \pi$, (b) results from algebraic manipulation after using some properties of Gamma function and $\mathbb{E}\left[{g_j}^{2/\alpha}\right] = \Gamma(1 + 2/\alpha)$.

Substituting (30), (32), (33) into (28) with $\delta = u_i^K T_v \|X_v\|^{\alpha} / P_v$ and we obtain the result.

B. PROOF OF $P_F(T_f, \alpha)$

Similar to the previous method of (28), the coverage probability of F-AP mode can be given as

$$\begin{aligned}P_f(T_f, \alpha) &= \Pr\left(\frac{P_f h_f \|X_f\|^{-\alpha}}{I_{l_0,fv} + I_{v,fv} + I_{f,fu}} \geq T_f\right) \\ &= \int_0^{\infty} Pr\left(h_f \geq \delta'\left(I_{l_0,fv} + I_{v,fv} + I_{f,fu}\right)\right) f_{\|X_f\|}\left(r_f\right) dr_f \\ &\overset{(a)}{=} \int_0^{\infty} \mathcal{L}_{I_{l_0,fv}}(\delta') \mathcal{L}_{I_{v,fv}}(\delta') \mathcal{L}_{I_{f,fv}}(\delta') f_{\|X_f\|}\left(r_f\right) dr_f \\ &\overset{(b)}{=} \int_0^{\infty} \exp\left(-\pi\lambda_f r_f^2 \rho\left(T_f, \alpha\right)\right) \\ &\quad \cdot \exp\left(-\pi\lambda_{tv}\Delta'(\alpha)\left(\delta' P_v\right)^{\frac{1}{\alpha}}\right) \\ &\quad \cdot \exp\left(-\pi^2\lambda_{tv}\lambda_l \Delta(\alpha)\left(\delta' P_v\right)^{\frac{2}{\alpha}}\right) 2\pi\lambda_f r_f e^{-\pi\lambda_f r_f^2} dr_f, \end{aligned} \tag{34}$$

where equation (a) follows channel fading $h_f \sim exp(1)$, $\delta' = T_f r_f^{\alpha} / P_f$ and the independence between inter-road interference $I_{l_0,fv}, I_{v,fv}$ and intra-road interference $I_{f,fv}$, (b) according to the definition of the Laplace transform for $I_{l_0,fv}$, $I_{v,fv}$ and $I_{f,fv}$, here $\mathcal{L}_{I_{l_0,fv}}$ and $\mathcal{L}_{I_{v,fv}}$ can be derived by using a similar way as (30) and (32), respectively.

And the $\mathcal{L}_{I_{f,fv}}$ can be further derived as

$$\begin{aligned}\mathcal{L}_{I_{f,fv}}(\delta') &= \mathbb{E}\left[\prod_{X_j'\in\Phi_f/f} \exp\left(-\delta' P_f g_j' \left\|X_j'\right\|^{-\alpha}\right)\right] \\ &= \exp\left(-2\lambda_f\pi \int_{\|X_f\|}^{\infty} \left(1 - e^{-\delta' P_f g_j' v^{-\alpha}}\right) v^2 dv\right) \\ &= \exp\left(-2\lambda_f\pi \int_{\|X_f\|}^{\infty} \frac{\delta' P_f}{1+\delta' P_f v^{-\alpha}} v^2 dv\right) \\ &\overset{(a)}{=} = \exp\left(-\pi\lambda_f r_f^2 \rho\left(T_f, \alpha\right)\right), \end{aligned} \tag{35}$$

where (a) follows from plugging in $\delta' = T_f r_f^{\alpha} / P_f$ and employing a change of variables $u = \left(v / \left(r_f T_f^{1/\alpha}\right)\right)^2$.

After using some algebraic manipulation (Please see [32, eq. (3.462)]), we obtain the close-form result and the proof is finished.

REFERENCES

[1] M. Boban, A. Kousaridas, K. Manolakis, J. Eichinger, and W. Xu,, "Connected roads of the future: Use cases, requirements, and design considerations for vehicle-to-everything communications," *IEEE Veh. Technol. Mag.*, vol. 13, no. 3, pp. 110–123, Sep. 2018.

[2] M. Fallgren *et al.*, "Fifth-generation technologies for the connected car: Capable systems for vehicle-to-anything communications," *IEEE Veh. Technol. Mag.*, vol. 13, no. 3, pp. 28–38, Sep. 2018.

[3] S. Chen, J. Hu, Y. Shi, and L. Zhao, "LTE-V: A TD-LTE-based V2X solution for future vehicular network," *IEEE Internet Things J.*, vol. 3, no. 6, pp. 997–1005, Dec. 2016.

[4] S. Chen *et al.*, "Vehicle-to-everything (V2X) services supported by LTE-based systems and 5G," *IEEE Commun. Standards Mag.*, vol. 1, no. 2, pp. 70–76, Jun. 2017.

[5] X. Ge, H. Chen, G. Mao, Y. Yang, and S. Tu, "Vehicular communications for 5G cooperative small-cell networks," *IEEE Trans. Veh. Technol.*, vol. 65, no. 10, pp. 7882–7894, Oct. 2016.

[6] C.-S. Choi and F. Baccelli, "Poisson Cox point processes for vehicular networks," *IEEE Trans. Veh. Technol.*, vol. 67, no. 10, pp. 10160–10165, Oct. 2018.

[7] C.-S. Choi and F. Baccelli, "An analytical framework for coverage in cellular networks leveraging vehicles," *IEEE Trans. Commun.*, vol. 66, no. 10, pp. 4950–4964, Oct. 2018.

[8] W. Sun, E. G. Ström, F. Brännström, K. C. Sou, and Y. Sui, "Radio resource management for D2D-based V2V communication," *IEEE Trans. Veh. Technol.*, vol. 65, no. 8, pp. 6636–6650, Aug. 2015.

[9] N. Cheng *et al.*, "Performance analysis of vehicular device-to-device underlay communication," *IEEE Trans. Veh. Technol.*, vol. 66, no. 6, pp. 5409–5421, Jun. 2017.

[10] S. Zhang, J. Chen, F. Lyu, N. Cheng, W. Shi, and X. Shen, "Vehicular communication networks in the automated driving era," *IEEE Commun. Mag.*, vol. 56, no. 9, pp. 26–32, Sep. 2018.

[11] M. Peng and K. Zhang, "Recent advances in fog radio access networks: Performance analysis and radio resource allocation," *IEEE Access*, vol. 4, pp. 5003–5009, Sep. 2016.

[12] M. Peng, S. Yan, K. Zhang, and C. Wang, "Fog-computing-based radio access networks: Issues and challenges," *IEEE Netw.*, vol. 30, no. 4, pp. 46–53, Jul./Aug. 2016.

[13] Z. MacHardy, A. Khan, K. Obana, and S. Iwashina, "V2X access technologies: Regulation, research, and remaining challenges," *IEEE Commun. Surveys Tuts.*, vol. 20, no. 3, pp. 1858–1877, 3rd Quart., 2018.

[14] F. Giust *et al.*, "Multi-access edge computing: The driver behind the wheel of 5G-connected cars," *IEEE Commun. Standards Mag.*, vol. 2, no. 3, pp. 66–73, Sep. 2018.

[15] C. Huang, R. Lu, and K.-K. R. Choo, "Vehicular fog computing: Architecture, use case, and security and forensic challenges," *IEEE Commun. Mag.*, vol. 55, no. 11, pp. 105–111, Nov. 2017.

[16] K. Zhang, Y. Mao, S. Leng, Y. He, and Y. Zhang, "Mobile-edge computing for vehicular networks: A promising network paradigm with predictive offloading," *IEEE Veh. Technol. Mag.*, vol. 12, no. 2, pp. 36–44, Jun. 2017.

[17] Z. Wang, Z. Zhong, D. Zhao, and M. Ni, "Bus-based cloudlet cooperation strategy in vehicular networks," in *Proc. IEEE VTC Fall*, Toronto, ON, Canada, Jun. 2018, pp. 1–6.

[18] Z. Hu, Z. Zheng, T. Wang, L. Song, and X. Li, "Roadside unit caching: Auction-based storage allocation for multiple content providers," *IEEE Trans. Wireless Commun.*, vol. 16, no. 10, pp. 6321–6334, Oct. 2017.

[19] M. Peng, Y. Li, J. Jiang, J. Li, and C. Wang, "Heterogeneous cloud radio access networks: A new perspective for enhancing spectral and energy efficiencies," *IEEE Wireless Commun.*, vol. 21, no. 6, pp. 126–135, Dec. 2014.

[20] M. Peng, K. Zhang, J. Jiang, J. Wang, and W. Wang, "Energy-efficient resource assignment and power allocation in heterogeneous cloud radio access networks," *IEEE Trans Veh. Technol.*, vol. 64, no. 11, pp. 5275–5287, Nov. 2015.

[21] M. Haenggi, *Stochastic Geometry for Wireless Networks*. Cambridge, U.K.: Cambridge Univ. Press, 2013.

[22] S. Yan, M. Peng, M. A. Abana, and W. Wang, "An evolutionary game for user access mode selection in fog radio access networks," *IEEE Access*, vol. 5, pp. 2200–2210, Mar. 2017.

[23] L. Breslau, P. Cao, L. Fan, G. Phillips, and S. Shenker, "Web caching and Zipf-like distributions: Evidence and implications," in *Proc. INFOCOM*, Mar. 1999, pp. 126–134.

[24] L. Duan, J. Huang, and B. Shou, "Economics of femtocell service provision," *IEEE Trans. Mobile Comput.*, vol. 12, no. 11, pp. 2261–2273, Nov. 2013.

[25] Y. Liu, L. Lu, G. Y. Li, Q. Cui, and W. Han, "Joint user association and spectrum allocation for small cell networks with wireless backhauls," *IEEE Wireless Commun. Lett.*, vol. 5, no. 5, pp. 496–499, Oct. 2016.

[26] S. Yan, M. Peng, and X. Cao, "A game theory approach for joint access selection and resource allocation in UAV assisted IoT communication networks," *IEEE Internet Things J.*, to be published. doi: 10.1109/JIOT.2018.2873308.

[27] W. Bao and B. Liang, "Rate maximization through structured spectrum allocation and user association in heterogeneous cellular networks," *IEEE Trans. Commun.*, vol. 63, no. 11, pp. 4510–4524, Nov. 2015.

[28] G. Hattab and D. Cabric, "Coverage and rate maximization via user association in multi-antenna HetNets," *IEEE Trans. Wireless Commun.*, vol. 17, no. 11, pp. 7441–7455, Nov. 2018.

[29] X. Yang and A. O. Fapojuwo, "Coverage probability analysis of heterogeneous cellular networks in Rician/Rayleigh fading environments," *IEEE Commun. Lett.*, vol. 19, no. 7, pp. 1197–1200, Jul. 2015.

[30] D. Stoyan, W. S. Kendall, and J. Mecke, *Stochastic Geometry and Its Applications*, 2nd ed. Hoboken, NJ, USA: Wiley, 1996.

[31] V. V. Chetlur and H. S. Dhillon, "Coverage analysis of a vehicular network modeled as Cox process driven by Poisson line process," *IEEE Trans. Wireless Commun.*, vol. 17, no. 7, pp. 4401–4416, Jul. 2018.

[32] I. S. Gradshteyn and I. M. Ryzhik, *Table of Integrals, Series, and Products*, 7th ed. New York, NY, USA: Elsevier, 2007.

SHI YAN received the Ph.D. degree in communication and information engineering from the Beijing University of Posts and Telecommunications, China, in 2017, where he currently holds a postdoctoral position with the Key Laboratory of Universal Wireless Communications, Ministry of Education. In 2015, he was an Academic Visiting Scholar with Arizona State University, Tempe, AZ, USA. His research interests include game theory, resource management, deep reinforcement learning, stochastic geometry, and fog radio access networks.

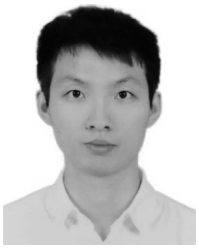

XINRAN ZHANG received the B.E. degree in communication and information engineering from Shandong University, China. He is currently pursuing the Ph.D. degree with the Beijing University of Posts and Telecommunications. His research interests include cooperative radio resource management and collaborative radio signal processing in vehicular networks.

HONGYU XIANG received the B.E. degree in telecommunication engineering from Fudan University, China, in 2013. He is currently pursuing the Ph.D. degree with the Beijing University of Posts and Telecommunications. His research interests include cooperative radio resource management and collaborative radio signal processing in heterogeneous cloud radio access networks and fog radio access networks.

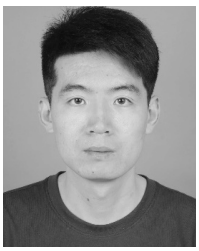

WENBIN WU received the B.E. degree in communication and information engineering from the Beijing University of Posts and Telecommunications, China, where he is currently pursuing the Ph.D. degree. His research interests include resource management and deep reinforcement learning in fog radio access networks.